ARTICLE
Journal of Cellular Biochemistry 108:134–144 (2009)

Journal of Cellular Biochemistry

On the Road to Understanding of the Osteoblast Adhesion: Cytoskeleton Organization Is Rearranged by Distinct Signaling Pathways

Willian Fernando Zambuzzi,[1*] Alexandre Bruni-Cardoso,[2] José Mauro Granjeiro,[3] Maikel Petrus Peppelenbosch,[4] Hernandes Faustino de Carvalho,[2] Hiroshi Aoyama,[1] and Carmen Veríssima Ferreira[1]

[1]*Department of Biochemistry, Biology Institute, University of Campinas, Campinas, São Paulo, Brazil*

[2]*Department of Cell Biology, Biology Institute, University of Campinas, Campinas, São Paulo, Brazil*

[3]*Department of Cell and Molecular Biology, Institute of Biology, Fluminense Federal University, Niterói, Rio de Janeiro, Brazil*

[4]*Kinome Profiling Unit, Department of Cell Biology, University Medical Center Groningen, University of Groningen, Groningen, The Netherlands*

ABSTRACT

Pre-osteoblast adhesion attracts increasing interest in both medicine and dentistry. However, how this physiological event alters osteoblast phenotype is poorly understood. We therefore attempted to address this question by investigating key biochemical mechanism that governs pre-osteoblast adhesion on polystyrene surface. Importantly, we found that cofilin activity was strongly modulated by PP2A (Ser/Thr phosphatase), while cell-cycle was arrested. Accordingly, we observed that the profile of cofilin phosphorylation (at Ser03) was similar to phospho-PP2A (at Tyr307). Also, it is plausible to suggest during pre-osteoblast adhesion that PP2A phosphorylation at Y307 was executed by phospho-Src (Y416). In addition, it was observed that MAPKp38, but not MAPK-erk, played a key role on pre-osteoblast adhesion by phosphorylating MAPKAPK-2 and ATF-2 (also called CRE-BP1). Also, the up-modulation of RhoA reported here suggests its involvement at the beginning of osteoblast attachment, while Akt remained active during all periods. Altogether, our results clearly showed that osteoblast adhesion is under an intricate network of signaling molecules, which are responsible to guide their interaction with substrate mainly via cytoskeleton rearrangement. J. Cell. Biochem. 108: 134–144, 2009.

KEY WORDS: PRE-OSTEOBLAST; ADHESION; PP2A; MAPKp38; COFILIN; Akt; SIGNAL TRANSDUCTION; ACTIN

Increased life expectancy poses new challenges to improve bone density control and fracture healing in both dental implantology and orthopedic applications [Logeart-Avramoglou et al., 2005; Kneser et al., 2006]. The ability of bone-cells to adhere and migrate in a temporal and spatially coordinated manner is critical for tissue morphogenesis, maintenance, and repair. The importance of osteoblast adhesion on material surfaces has been evidenced, but few advances have been achieved in order to explain how these events occur. Together, cell adhesion and proliferation represent the first steps of cell–biomaterial interactions and their efficacy influence the subsequent ability to differentiate [Choi et al., 2005; Müller et al., 2008]. In fact, Müller et al. [2008] propose that calcium phosphate surfaces are able to drive mesenchymal stem cells differentiation into osteoblasts and that a dynamic behavior of focal adhesions might be involved in the molecular mechanisms promoting osteogenic differentiation.

In general, when eukaryotic cells adhere on different substrata important intracellular mechanisms are triggered mainly upon integrin activation, since these receptors bridge the cell surface and the extracellular matrix (ECM) components such as collagens and fibronectin. In addition to the adhesive functions, integrin mediates

Additional Supporting Information may be found in the online version of this article.

Grant sponsor: Fundação de Amparo a Pesquisa do Estado de São Paulo (Fapesp); Grant number: 08/53003-9.

*Correspondence to: Willian Fernando Zambuzzi, PhD, Division of Cell signaling and Biossays, University of Campinas, Cidade Universitária "Zeferino Vaz," Campinas, SP 13083-970, Brazil. E-mail: wzamba@unicamp.br

Received 26 February 2009; Accepted 7 May 2009 • DOI 10.1002/jcb.22236 • © 2009 Wiley-Liss, Inc.
Published online 26 June 2009 in Wiley InterScience (www.interscience.wiley.com).

both inside-out and outside-in signaling between the ECM and the cell [Zambuzzi et al., 2009].

Upon integrin activation, cytoskeleton and signaling molecules are recruited into focal adhesion structures, promoting transient focal adhesion kinase (FAK) phosphorylation at tyrosine residues (Y). Afterwards, these signaling mechanisms are responsible for the cytoskeleton rearrangement executed by cofilin, which interacts directly with actin (monomer or filaments). A dynamic actin-cytoskeleton is essential for a wide variety of normal cellular processes, including the maintenance of cell shape and migration [Müller et al., 2008; Myers and Casanova, 2008]. Therefore, cofilin plays pivotal roles in cytokinesis, endocytosis, embryonic development, stress response and tissue regeneration [Carlier et al., 1999]. In response to diverse stimuli, cofilin promotes the regeneration of actin filaments by severing preexisting fibers [Condeelis, 2001].

Initial steps of pre-osteoblast adhesion are important for improving the biocompatibility of biomaterials [Hamilton and Brunette, 2007]; however, how this physiological event alters osteoblast phenotype is poorly understood. We therefore attempted to address this question by investigating key biochemical mechanism that governs pre-osteoblast adhesion on polystyrene surface, mainly by affecting actin-filaments remodeling. Summarizing, our findings suggest that the cytoskeleton rearrangement required during pre-osteoblast adhesion is governed by distinct signaling mediators such as cofilin, MAPKAPK-2/HSP27, and RhoA. In addition, we noticed that cell-cycle was arrested at the beginning of the process, while Akt remained active. Finally, we showed that PP2A (Ser/Thr phosphatase) and MAPKp38 are able to dephosphorylate cofilin and phosphorylate MAPKAPK-2, respectively. To our knowledge, we demonstrated, for the first time, a link between these components and actin-filaments remodeling during pre-osteoblast adhesion. Certainly, these results are relevant to a better understanding of the molecular mechanism underlying the behavior of pre-osteoblasts in bone regenerative (oral and orthopedic) procedures.

MATERIALS AND METHODS

ANTIBODIES AND DRUGS

β-Actin, p-MAPKp38 (Thr180), p-Akt (Tyr326), p-ATF-2 (Thr69), p-MAPKAPK-2 (Thr222), p-Cofilin (ser03), anti-mouse, anti-rabbit, and anti-goat IgGs antibodies were purchased from Cell Signaling Technology (Boston, MA). Anti-p-PP2A (Tyr307) antibody was from Santa Cruz Biotechnology (Santa Cruz, CA). Enzyme inhibitors [SB203580, PD098059, Okadaic Acid (Oka)] were from Sigma Chemical Co. (St. Louis MO).

CELL LINE AND CULTURE CONDITIONS

MC3T3-E1 cells (sub-clone 4), a mouse pre-osteoblast cell line, were obtained from American Type Culture Collection (ATCC, Rockville, MD) and grown at 37°C in α-MEM medium supplemented with 10% FBS, 100 U/ml of penicillin, and 100 μg/ml of streptomycin under a humidified 5% CO_2 atmosphere.

EXPERIMENTAL DESIGN

In order to assess the biochemical behavior of pre-osteoblast adhesion on polystyrene surfaces, MC3T3-E1 cells were seeded on polystyrene surfaces and the samples collected after 1, 6, 24, and 48 h of culturing.

PRE-OSTEOBLAST ADHESION AND PROLIFERATIVE ASSAYS

Pre-osteoblast adhesion and proliferation rate were assessed by colorimetric assays using crystal violet as described previously [Brasaemle and Attie, 1988] with slight modifications and MTT reduction [Mosmann, 1983], as described below.

CRYSTAL VIOLET STAINING

One milliliter of MC3T3-E1 cells were seeded at 5×10^4 cells/ml in 24-well culture plates for 1, 6, 24, and 48 h. Briefly, adherent cells were rinsed in warm PBS and fixed in absolute ethanol-glacial acetic acid (3:1; v/v) for 10 min at room temperature and air dried (eventually stored at 4°C, wrapped in aluminum foil). The adherent cells were stained with 0.1% crystal violet (w/v) for 10 min at room temperature. Excess dye was removed by decantation and washed twice with distilled water. The dye was extracted with 10% acetic acid (v/v), and the optical density measured at 550 nm using a microplate reader (Biotek Co., Winooski, VT). Data from each experiment were analyzed with six observations in each group.

MTT REDUCTION

MC3T3-E1 cells were seeded at 5×10^4 cells/ml in 24-well culture plates for 1, 6, 24, and 48 h. Cell proliferation was assessed by a colorimetric assay using 3-[4,5-dimethylthiazol-2-yl]-2,5-diphenyltetrazolium bromide (MTT). Briefly, the culture medium was removed and 1 ml MTT solution (1 mg MTT/ml of culture medium) was added to each well and incubated for 3 h at 37°C. After incubation, the MTT solution was removed and the formazan solubilized in 1 ml of DMSO. The plate was shaken for 5 min on a plate shaker (Biotek Co.) and the absorbance measured at 570 nm using a microplate reader (Biotek Co.).

MAPKS AND PP2A ACTIVITY INHIBITION ASSAY USING CLASSICAL INHIBITORS

Ten milliliters of MC3T3-E1 cells (5×10^4 cells/ml) were seeded on cell culture dishes (10 cm of diameter), 1 h after seeding the cells were incubated with medium containing specific inhibitor (SB203580 or PD098059 or Oka) for 2 h. Next, the adherent cells were lyzed and pool of proteins were collected and resolved by SDS–PAGE and transferred to PVDF membrane as bellow described for immunoblotting. The inhibitors concentrations carried in our experiments were from literature data and did not promote cytotoxicity on MC3T3-E1 cells up 24 h of treatment (data not shown). Inhibitor concentrations employed in this work were: SB 203580 (MAPKp38), 5 μM; PD 098059 (ERK), 5 μM; Okadaic Acid (PP2A), 10 nM.

CELL RECOVERING AFTER P38 INHIBITION

In order to check the viability of cells, which did not attach on polystyrene when were pre-treated with p38 inhibitor (SB203580), a cell recovering assay was performed. Before experimentation,

MC3T3-E1 cells were treated with SB203580 exactly as described previously. Cells which did not attach on the polystyrene (in suspension) were collected by centrifugation at 2,610*g*. Afterwards, the pellet of cells was resuspended and washed twice with warm PBS, the cells were centrifugated again and cell pellet resuspended in complete α-MEM without p38 inhibitor. Subsequently, cells taken from the pellet were counted using a hemocytometer chamber and re-seeded (7×10^4 cells/ml) in 24-well plates and cultured for 1, 2, 3, 6, 12, and 72 h. Hereafter, the attached cells were assessed by crystal violet dye and the cells which did not attach were assessed by the trypan blue dye exclusion.

PHOSPHOMAPKAPK-2 IN THE NUCLEUS COMPARTMENT

Ten milliliters of MC3T3-E1 cells (5×10^4 cells/ml) were seeded on 10 cm-diameter dish plates. One hour after seeding, the cells were washed (ice-cold PBS) and scraped into 100 μl ice-cold cell extract buffer [10 mM HEPES–KOH (pH 7.9), 1.5 mM $MgCl_2$, 10 mM KCl, 0.5 mM dithiothreitol (DTT) and 0.2 mM phenylmethylsulfonyl fluoride (PMSF)]. The pellet of cells was kept on ice for 10 min, vortexed for 10 s, and centrifuged at 4°C for 30 s at 18,000*g*. The supernatant was discarded and the pellet was resuspended in 30 μl of nuclear extraction buffer [20 mM HEPES–KOH (pH 7.9), 25% glycerol, 420 mM NaCl, 1.5 mM $MgCl_2$, 0.2 mM EDTA, 0.5 mM DTT, and 0.2 mM PMSF], placed on ice for 20 min, and centrifuged at 4°C for 2 min at 18,000*g*. The supernatant was saved as nuclear extract and pMAPKAPK-2 checked by immunoblotting assay.

IMMUNOBLOTTING ASSAY

MC3T3-E1 pre-osteoblast cells were cultured and protein extracts were obtained using Lysis Cocktail (50 mM Tris [tris(hydroxymethyl)aminomethane]-HCl [pH 7.4], 1% Tween-20, 0.25% sodium deoxycholate, 150 mM NaCl, 1 mM ethylene glycol tetraacetic acid (EGTA), 1 mM *O*-Vanadate, 1 mM NaF, and protease inhibitors [1 μg/ml aprotinin, 10 μg/ml leupeptin, and 1 mM 4-(2-aminoethyl)-benzolsulfonyl-fluorid-hydrochloride]) for 2 h on ice, as used previously. After clearing by centrifugation, the protein concentration was determined using Lowry method [Hartree, 1972]. An equal volume of 2× sodium dodecyl sulfate (SDS) gel loading buffer (100 mM Tris-HCl [pH 6.8], 200 mM dithiothreitol [DTT], 4% SDS, 0.1% bromophenol blue, and 20% glycerol) was added to samples and boiled for 5 min. Proteins extracts were resolved by SDS–PAGE (10% or 12%) and transferred to PVDF membranes (Millipore). Membranes were blocked with either 1% fat-free dried milk or bovine serum albumin (2.5%) in Tris-buffered saline (TBS)—Tween-20 (0.05%) and incubated overnight at 4°C with appropriate primary antibody at 1:1,000 dilutions. After washing in TBS–Tween-20 (0.05%), membranes were incubated with horse radish peroxidase-conjugated anti-rabbit, anti-goat or anti-mouse IgGs antibodies, at 1:2,000 dilutions (in all immunoblotting assays), in blocking buffer for 1 h. Detection was performed by using enhanced chemiluminescence.

IMMUNOFLUORESCENCE MICROSCOPY

In order to detect phospho-cofilin or actin filaments, MC3T3-E1 pre-osteoblast cells were placed on untreated polystyrene discs and incubated at 37°C for 1, 6, 24, and 48 h. Adherent cells were then fixed with 1% paraformaldehyde in phosphate-buffered saline (PBS) and permeabilized with 0.1% Triton X-100 for 30 min. After washing twice with PBS, cells were incubated in 10% BSA/PBS for 1 h. Primary antibodies were diluted in PBS/BSA plus 0.01% Triton X-100. The cells were incubated with anti-phospho-cofilin antibody (1:50 dilution) overnight. Afterwards, an extensive washing with PBS was made, and the cells incubated with FITC-conjugated anti-rabbit immunoglobulin G at a 1:750 dilution. In some cases, actin filaments were also labeled with rhodamine TRITC-conjugated phalloidin (1:40) for 30 min. All the antibodies were diluted in PBS containing 0.5% BSA. Images were then imported into Adobe Photoshop for cropping.

STATISTICAL ANALYSIS

All experiments were performed in triplicates and the results shown in the graphs represent the mean ± standard error of the mean (SEM). Data from each assay were analyzed statistically by ANOVA. Differences were considered significant when the $P < 0.05$. Immunoblottings represent three independent experiments. We used Image Pro-Plus to analyze the densitometry of bands from immunoblottings (arbitrary values).

RESULTS

DYNAMICS OF ACTIN REARRANGEMENT CONTROL CELL MORPHOLOGY DURING PRE-OSTEOBLAST ADHESION

Based on phalloidin staining, the Figure 1C shows that cell-shape was changed during pre-osteoblast adhesion, and it was associated with actin-filaments rearrangement.

Data from our experimental model support that these events can be divided into three phases: adhesion (1 h), spreading (<6–24 h) and later, proliferative phase (at 48 h). Importantly, at 24 h it was possible to note the occurrence of self-rearrangement of cellular morphology (arrows, Fig. 1C). Next, we identified several cell signaling pathways involved in the cell-shape changes along the pre-osteoblast adhesion, spreading and proliferation.

CELL-CYCLE WAS ARRESTED DURING PRE-OSTEOBLASTS ADHESION

Proliferation rate was not linear up to 24 h as demonstrated by different index (Fig. 1A). In order to evaluate the effect of polystyrene surface at the proliferation rate of MC3T3-E1 cells, cell-cycle regulators were assessed by immunobloting analysis. The results revealed activation of cell proliferation inhibitors at the early adhesion phase (1 h) as compared to later stages (6, 24, and 48 h). Strategically, we assessed biochemical markers such as cdk4, cyclinD1, p15, p21 and cdc2, which are responsible for controlling the cell-cycle progression. Figure 1B shows that cdk4 and cyclinD1 were down-regulated while $p21^{Cip/WAF1}$, $p15^{INK4B}$, and p-cdc2 (tyr15, inhibitory site) were up-regulated on early periods (1 and 6 h). These results clearly show that cell-cycle was arrested during the early stages of pre-osteoblast adhesion. On the other hand, Akt remained active (phosphorylated) throughout the experimental periods (Fig. 2), reinforcing the viability of cells.

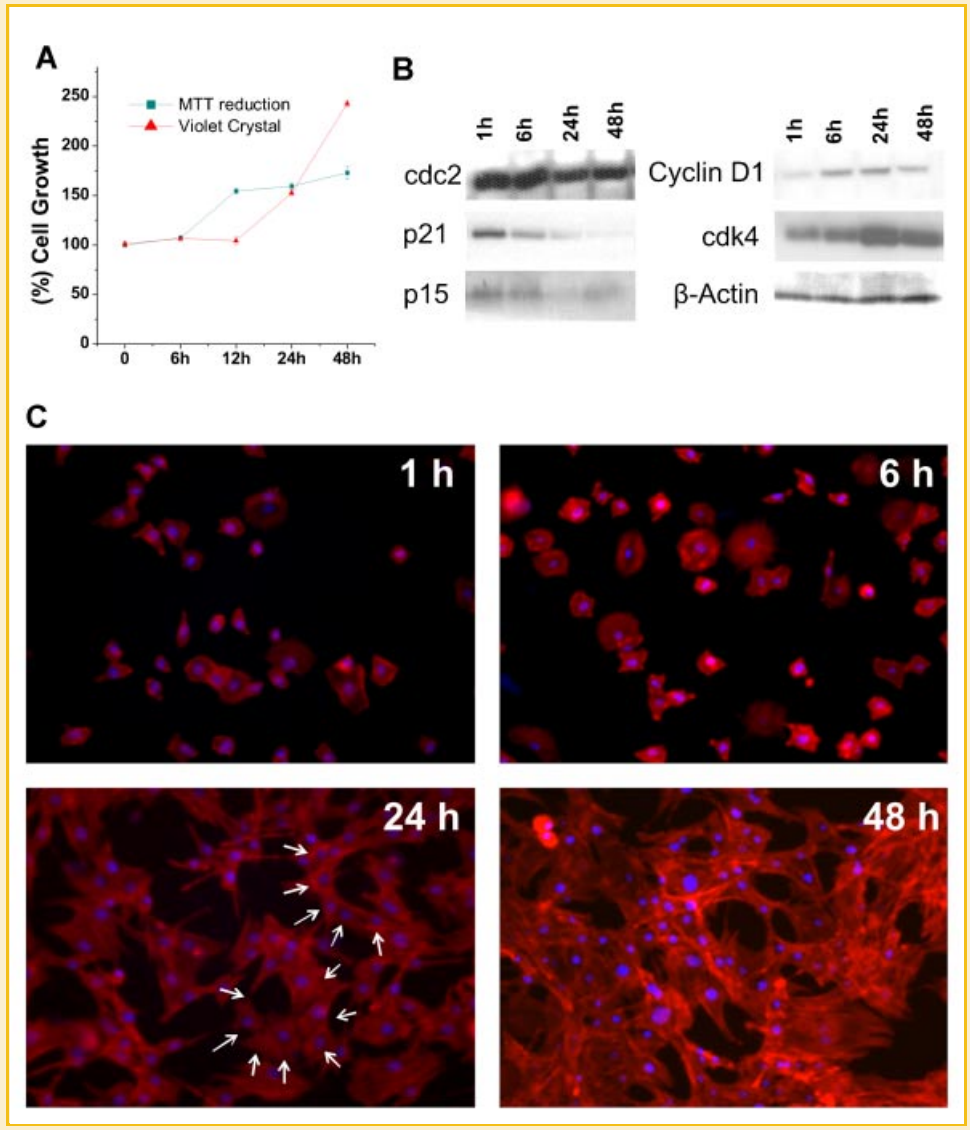

Fig. 1. Actin-filaments staining and proliferation kinetics during osteoblasts adhesion. A: Cell viability was assessed by MTT or Violet crystal (VC) relative to time 0 (100%) ($P < 0.05$). B: Key modulators expression of cell-cycle progression (cdk4, cyclinD1, p21, p15, and cdc2). C: Cellular morphological changes were assessed by staining with TRITC-phalloidin (red). Nuclei were stained by DAPI (blue). Magnification: 100×. [Color figure can be viewed in the online issue, which is available at www.interscience.wiley.com.]

TYROSINE AND THREONINE PHOSPHORYLATION LEVELS DURING PRE-OSTEOBLAST ADHESION

To assess the baseline of protein phosphorylation, MC3T3-E1 pre-osteoblast cells were grown on polystyrene surfaces for 1 or 48 h and samples were collected for immunoblotting analysis. The same amount of proteins was resolved for both and the comparison between these two conditions showed that phosphorylation levels of both phosphorylation sites (Y or Thr) changed during the pre-osteoblast adhesion and proliferation. Proteins phosphorylated at tyrosine residue were more evident at 1 h than 48 h after seeding (Fig. 3). On the other hand, more protein bands phosphorylated at threonine were detected at 48 h than at 1 h. With these findings, we can speculate that protein tyrosine kinases (PTKs) play an important role at the beginning of osteoblast adhesion.

PP2A MODULATES COFILIN FUNCTION BY DEPHOSPHORYLATING SERINE-03

Our result from immunoblotting data showed an increase in cofilin phosphorylation (Fig. 4B) with concomitant rise of the phosphorylation level at the inhibitory site of PP2A (Y307, showed in Fig. 4A) up to 48 h of seeding. In addition, the difference of cofilin phosphorylation was checked by immunoflorescence between 1 and 48 h (right panel) and in accordance, phosphorylated cofilin at ser 03 was also observed to be higher at 48 h in relation to 1 h. In addition, concomitantly with PP2A phosphorylation (Y307), we showed that Src activity (checked by phospho-Y416) was increased up to 48 h (Fig. 5B). In order to establish the possible connection between PP2A activity and cofilin activation, we checked phospho-cofilin in pre-osteoblasts treated with 10 nM okadaic acid

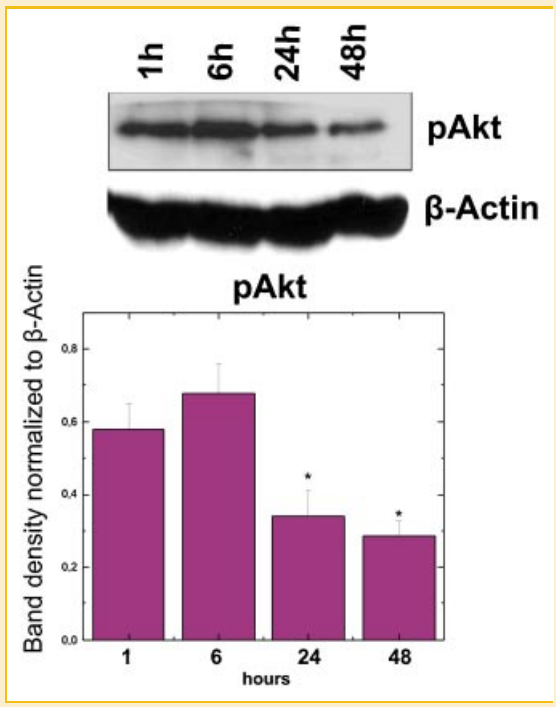

Fig. 2. Protein kinase Akt phosphorylation analysis throughout adhesion, and proliferation of pre-osteoblasts. Phosho-Akt was checked through immunoblotting using specific antibody against the Y326 phosphorylated form. The graphs represent plots of means ± standard error of the means of intensities (minus background) from the region of interest using data from three separate experiments ($^*P < 0.05$). Band density was normalized to β-actin. [Color figure can be viewed in the online issue, which is available at www.interscience.wiley.com.]

(a concentration showed to be non-toxic for MC3T3-E1 cells, data not shown). As expected, this experiment showed that the inhibition of PP2A guaranteed high levels of phosphorylated cofilin (Fig. 4C). In this way we can speculate that PP2A is responsible for keeping cofilin in the active state by dephosphorylation at Serine 03. Accordingly, cell-shape and actin rearrangement were affected by OKA treatment (Fig. 4E, left panel). In addition, in order to investigate the distribution of phospho-cofilin in intact cells we used immunofluorescence (Fig. 4E, middle panel) and determined that phospho-cofilin was associated with less adherent rounded cells and less stress fibers. Therefore, our findings indicated that the modulation of cofilin by PP2A contributes for pre-osteoblast adhesion (Fig. 4D).

BOTH FAK AND RhoA CONTRIBUTE TO CYTOSKELETON REMODELING

As maximal Y-phosphorylation was observed at 1 h after seeding (Fig. 2), specific PTKs became a strategically target for investigation. Thus, focal adhesion kinase (FAK) was assessed at this time point. We found that FAK (at Y397) was up-phosphorylated at 1 h, (Fig. 5A). Additionally, the examination of RhoA expression demonstrated that this protein was tightly regulated during pre-osteoblast adhesion, up to 6 h after cell seeding (Fig. 5A). Also, Src (pY416) remained active during all periods (Fig. 5B).

ATF-2 AND MAPKAPK-2 ARE PHYSIOLOGICAL SUBSTRATES FOR MAPKp38, BUT NOT FOR ERK

Our experiments clearly showed that MAPKp38 is required and probably plays an important role in pre-osteoblast adhesion, since this kinase remained active up to 6 h after pre-osteoblast seeding (Fig. 6). In agreement with this result, we also observed that ATF-2 and MAPKAPK2, two potential physiological substrates of

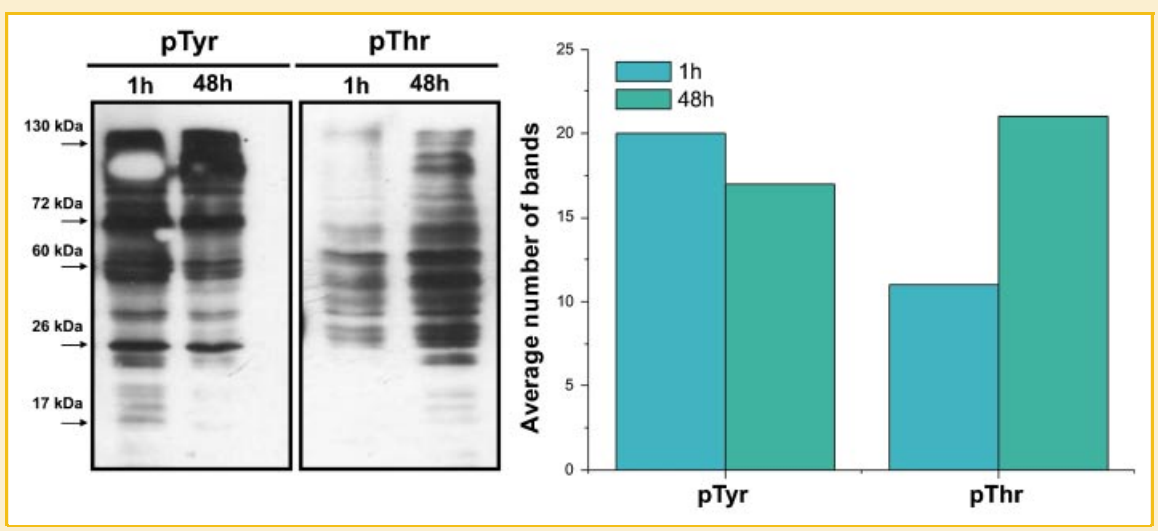

Fig. 3. Pre-osteoblasts adhesion-induced changes in phosphorylation state of tyrosine (pTyr) and threonine (pThr). Immunoblotting using specific antibody against pTyr and pThr form were used. The data shown in (A) is graphically represented in (B). The same amount of protein was resolved in each lane. [Color figure can be viewed in the online issue, which is available at www.interscience.wiley.com.]

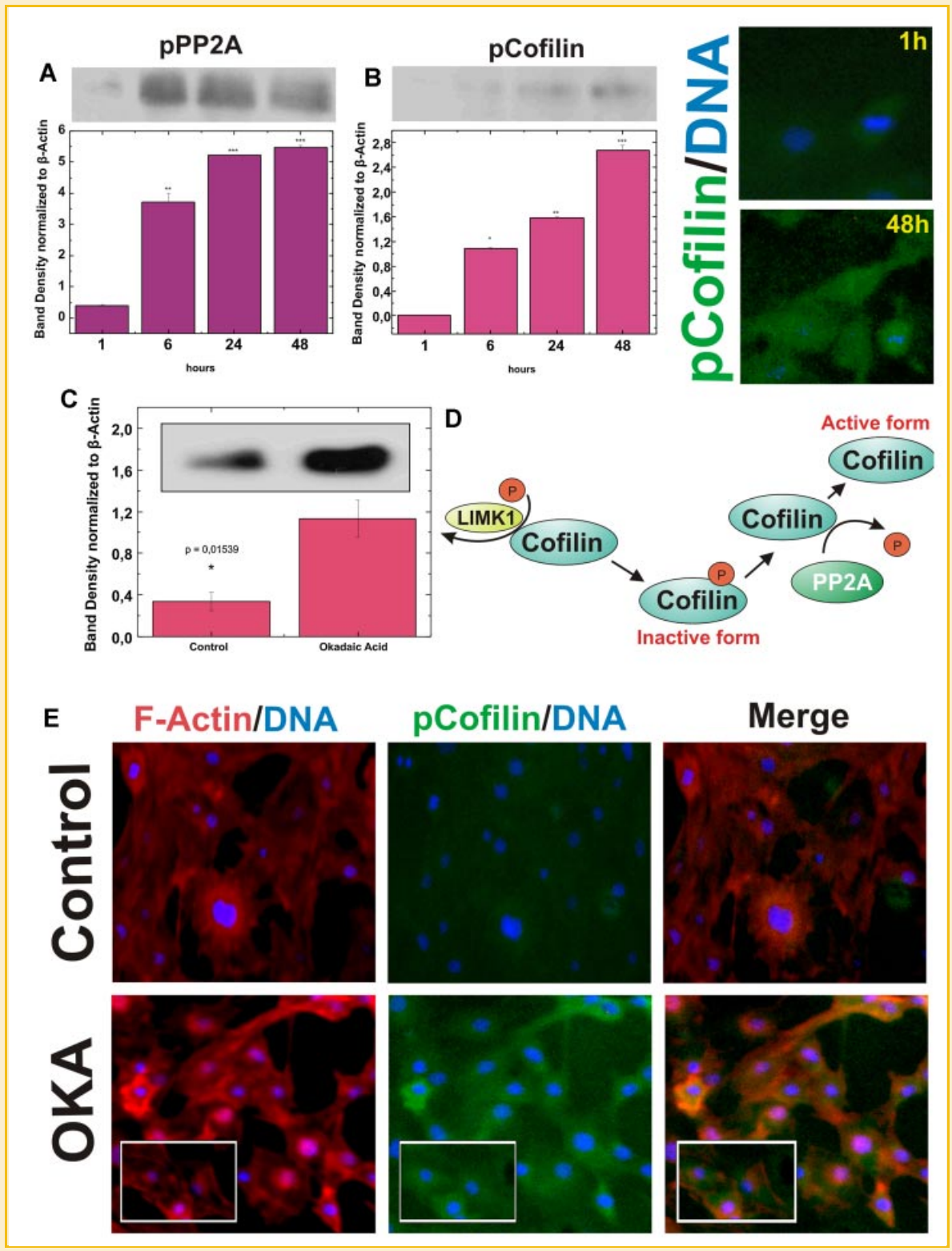

Fig. 4. Dephosphorylation of p-cofilin by PP2A during pre-osteoblasts adhesion. Phosphorylation of PP2A (A) and Cofilin (B) were evaluated by immunoblotting. The immunoflorescence label supported these results (right panel, *top*). C: PP2A inhibition with Oka resulted in an increased cofilin phosphorylation ($P = 0.015$). D: Diagram showing the biochemical mechanisms required for modulation of cofilin activity, pointing out PP2A as an important regulator of its activity. E: Cells were treated with Oka (10 nM) for 2 h and morphological differences between them were checked. Protein loading was assessed by probing β-actin, which was also used to normalize band intensity. [Color figure can be viewed in the online issue, which is available at www.interscience.wiley.com.]

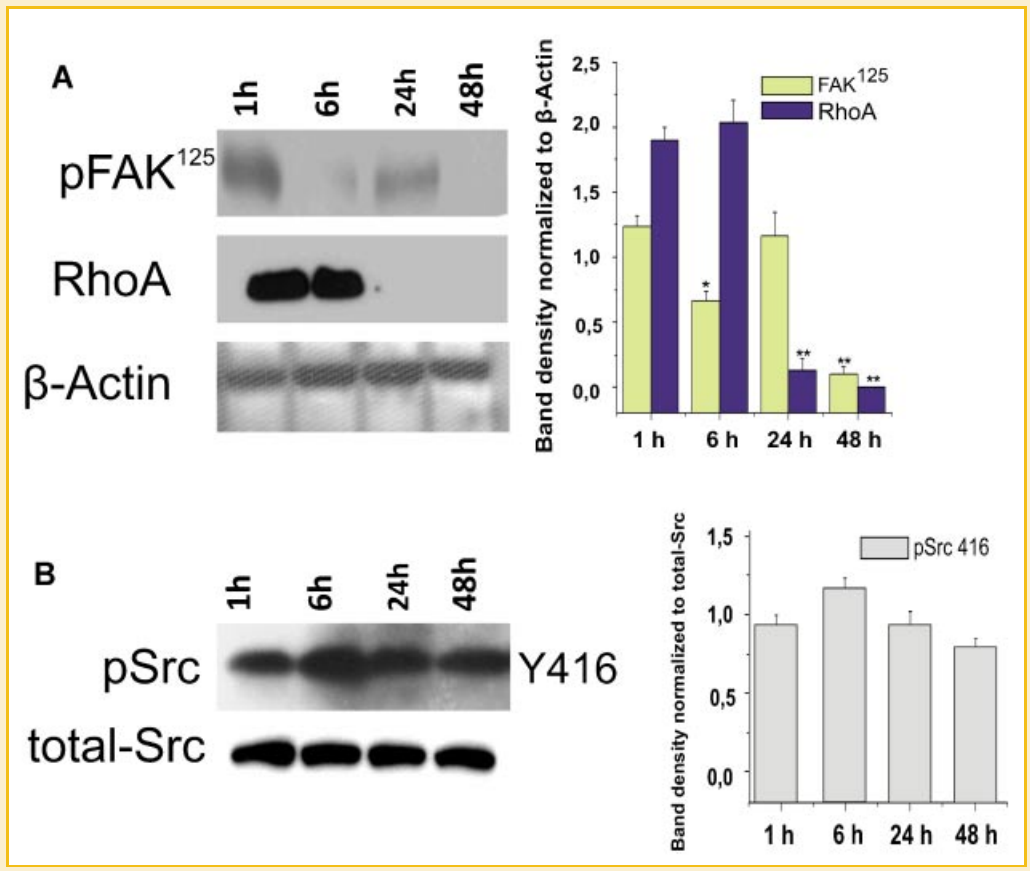

Fig. 5. FAK^{p125} and GTPase-RhoA are required at the beginning of pre-osteoblast adhesion (A), while Src (pY416) is remained active (B). Statistical comparison was made between groups with significance selected at $^{*}P < 0.05$ or $^{**}P < 0.01$. [Color figure can be viewed in the online issue, which is available at www.interscience.wiley.com.]

MAPKp38, were phosphorylated when MAPKp38 was more active (1 and 6 h) (Fig. 6). In order to verify the importance of MAPKp38 for pre-osteoblast adhesion, the adherent cells were treated with classical MAPKp38 inhibitor (SB203580) or MAPK Erk inhibitor (PD059038) for 2 h. We found that phosphorylation of ATF-2 (Fig. 7A) and MAPKAPK-2 (Fig. 7A) levels dropped significantly ($P < 0.05$) in the presence of MAPKp38 inhibitor (SB203580), but no effect was observed when MAPK Erk was inhibited. To validate

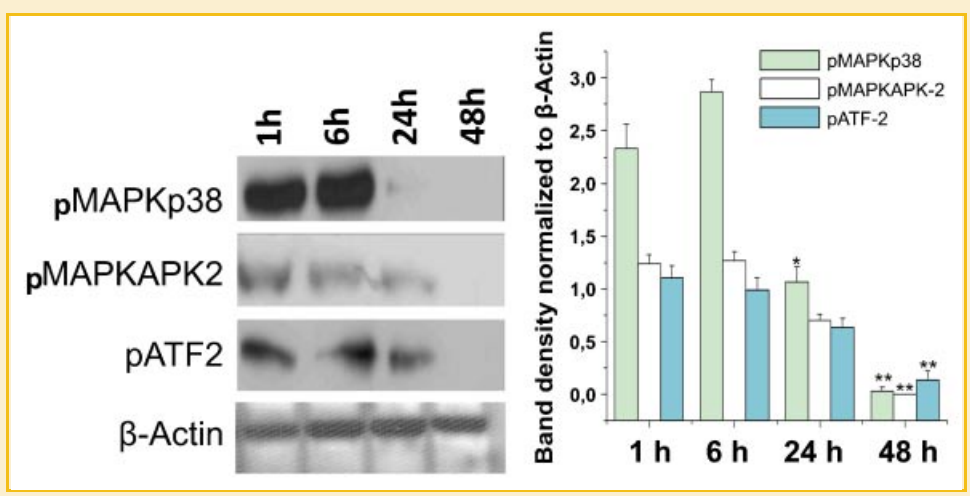

Fig. 6. Phosphorylation profile of MAPKp38 (Thr180), MAPKAPK-2 (Thr222) and ATF-2 (Thr69) during pre-osteoblast adhesion. The phosphorylation status was assessed by immunoblotting. $^{*}P < 0.05$ or $^{**}P < 0.05$. Band density was normalized to β-actin. [Color figure can be viewed in the online issue, which is available at www.interscience.wiley.com.]

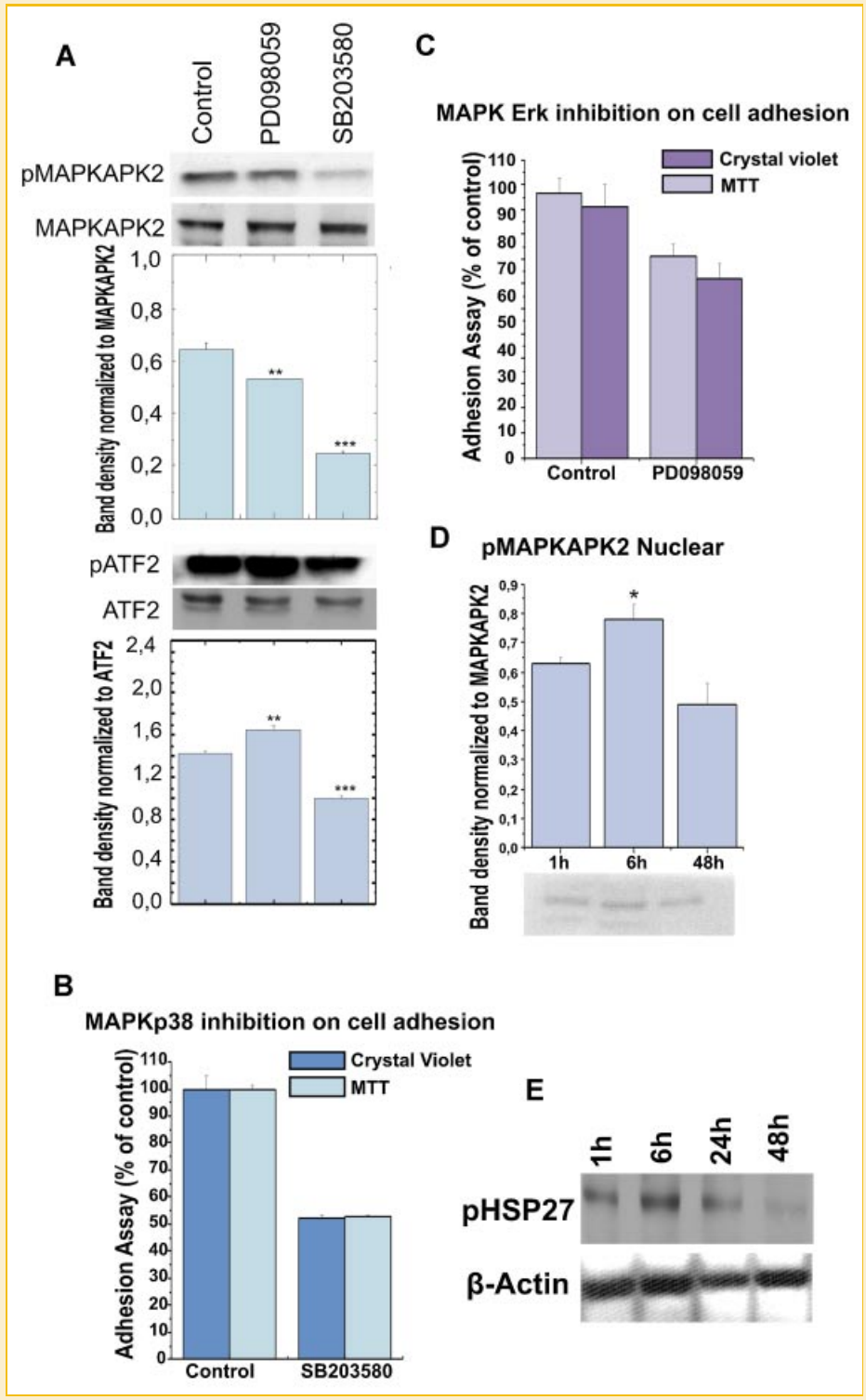

Fig. 7. MAPKAPK2 and ATF 2 are physiological substrates for MAPKp38, but not for MAPK erk, during pre-osteoblast adhesion. Phosphorylation level of ATF-2 (A, top) and MAPKAPK2 (A, bottom) was analyzed. $^{**,***}P < 0.05$. Influence of MAPK inhibitors on pre-oesteoblasts adhesion: MAPKp38 (B) and ERK (C). pMAPKAPK-2 (at thr222) translocates to the cell nucleus (D). HSP27 phosphorylation profile (E). Protein loading was assessed by probing β-actin, which was also used to normalize band density. [Color figure can be viewed in the online issue, which is available at www.interscience.wiley.com.]

the hypothesis that MAPKAPK-2 was activated via phosphorylation, we investigated whether phosphoMAPKAPK-2 was translocated to the cell nucleus. Figure 7D shows that MAPKAPK-2 was phosphorylated into nucleus in all periods evaluated, though it appeared higher up to 6 h. We also investigated the possibility of HSP27 to modulate the cytoskeleton rearrangement upon MAPKAPK2 activation. Despite being HSP27 phosphorylated during all period examined, it was higher at the early cell adhesion phase (Fig. 7E).

Still to prove the importance of MAPKp38 for modulating cell adhesion, we treated MC3T3-E1 cells with MAPKp38 inhibitor (in the same conditions described previously), afterwards, the adherent cells were detached and re-plated on polystyrene surfaces. Importantly, we reported that MAPKp38 inhibitor affected about 50% of the cells adhesion (MTT: 52.4%; crystal violet: 52.8%), which did not attach on substrate (Fig. 7B), while MAPK Erk inhibition was less effective, that is, only 20% of the cells did not adhere (Fig. 7C). In addition, we checked the viability of the cells which did not attach after treatment with p38 inhibitor (cell recovering assay). We observed that these cells were able to adhere and proliferate up to 72 h and importantly, cell death was not observed up to 72 h (Supplementary Fig. 1).

Figure 8 shows a general overview of signal pathways addressed in this study. It is noteworthy that actin-filaments were remodeled by distinct mediators. It is also noticeable that MAPKp38 plays a crucial role for cell adhesion.

DISCUSSION

Amongst the myriad observations on the influence of substratum on cell behavior, intracellular signal transduction has received relatively little attention. Cell adhesion to material surfaces is one of the fundamental phenomena of cellular response to implanted devices into bone and tooth lesions. Accordingly, "next generation" dental/orthopedic biomaterials should be able to promote pre-osteoblast adhesion thus improving the integration process between surgically placed implants and biological tissues. Also in this sense, it is known that surface properties influence cell adhesion, morphology changes and function [Bertazzo et al., 2009], however, how these events are governed by signaling pathways remains poorly understood.

In this work, we observed that proteins related to cell-cycle progression were specific and tightly modulated during pre-osteoblast adhesion. It was showed that cell-cycle arrest is an obligatory prerequisite for initial steps of cell attachment. Based on our results, it was able to define that p15/p21 ratio and cyclinD1 modulators were increased at G_0-phase, while cdk4 was down-regulated at 1 h of seeding. Physiologically, it seems that the low cell proliferation rate at early phase adhesion is also attributed to a negative modulation of adhesion-induced signaling, once that cell adhesion signaling is one of prerequisites for increasing cell-cycle progression. Importantly, we reported that Akt remained active along the adhesion period analyzed, which indicated that besides

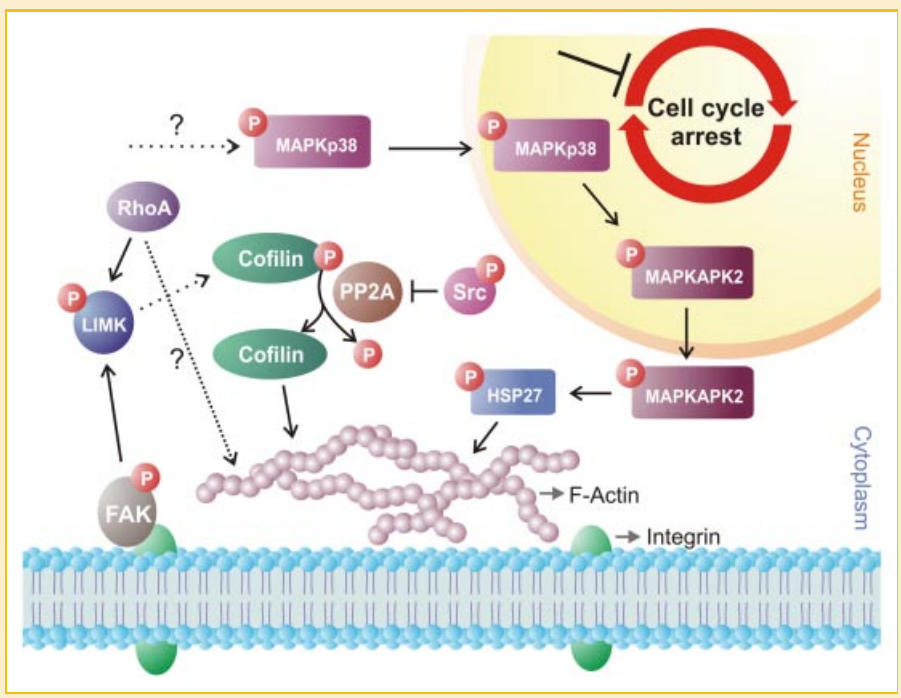

Fig. 8. Schematic representation of the biochemical mechanisms that govern pre-osteoblast adhesion. We defined that distinct pathways were involved during pre-osteoblast adhesion resulting cytoskeleton remodeling. Upon integrin (int) activation, signaling molecules are recruited into focal adhesion structures, promoting transient focal adhesion kinase (FAK) phosphorylation and its responsible for activating new signaling proteins, such as LIMK (downstream targets). In response to stimuli, cofilin promotes the regeneration of actin filaments by severing preexisting filaments (actin-rearrangement). Cell cycle was arrested during earlier processes involved with osteoblast attachment. Altogether, these molecular mechanisms described in this article are crucial for pre-osteoblast adhesion. [Color figure can be viewed in the online issue, which is available at www.interscience.wiley.com.]

inhibition of the cell-cycle progression, pre-osteoblasts signaling survival pathways were kept active.

Phosphorylation at Y is generally accepted as a critical regulator of a multitude of cell biological processes including cell proliferation, migration, differentiation, survival signaling and energy metabolism [Ferreira et al., 2006]. Accordingly, activation and recruitment of paxilin, Src, focal adhesion kinase (FAK), and vinculin to focal adhesions are associated with an increase in tyrosine phosphorylation. Phosphorylation of these proteins creates docking sites for the activation of other cytosolic protein kinases/phosphatases involved in migration, cytoskeletal organization, gene expression, and cell-cycle progression [Fincham et al., 2000]. In fact, our results demonstrated that actin-filaments remodeling is crucial at the beginning of pre-osteoblast adhesion and that it was governed by distinct pathways. For instance, during pre-osteoblast adhesion, we showed RhoA activation up to 6 h is an important mediator, once RhoA has been shown to induce actin-polymerization [Paterson et al., 1990; Ridley and Hall, 1992], although it is still unclear whether this protein is localized in focal adhesions [Adamson et al., 1992].

Interestingly, we observed that PP2A (Ser/Thr protein phosphatase) was expressively phosphorylated at its inhibitory site after 6 h of cell seeding on polystyrene surfaces. In addition, we detected that Src kinase was more active in these cells. Chen et al. [1992] reported that Src kinase is able to negatively modulate PP2A via phospharylation of its inhibitory site. More recently, our group has shown that MC3T3-E1 is able to express Src, which plays a crucial role during their differentiation [Zambuzzi et al., 2008]. It is clear that this transient deactivation of PP2A might enhance transmission of cellular signals through kinase cascades within cells.

Importantly, the PP2A inhibition was in agreement with the increase of phosphorylated cofilin (at Ser03), which we predicted as a potential physiological substrate of PP2A. Since the treatment of the cells with Oka caused a dramatically increase of the phosphorylation of cofilin, it is an indication that cofilin is a substrate of PP2A in those cells. This observation brought out new biochemical details for the modulation of cofilin activity in eukaryotic cells, at least regarding to pre-osteoblast adhesion on polystyrene surfaces. In this context, cofilin modulation turned out as an important player in regulating the dynamics of actin, by defining the average length of actin filament. Therefore, it is clear that the maintenance of inative cofilin (phosphorylated form) via inhibition of PP2A is important for triggering actin rearrangement during the early pre-osteoblast adhesion on polystyrene surfaces.

In this work, we also reported that both MAPKAPK-2 and ATF-2 are down-stream substrates of MAPKp38, but not of MAPK Erk, during pre-osteoblast attachment. It is known that when phosphorylated, MAPKAPK-2 is responsible for collaborating to actin-filaments rearrangement by phosphorylating HSP27 [Lavoie et al., 1993; Rousseau et al., 1997]. To validate this signaling mechanism, we evaluated the presence of phosphoMAPKAPK-2 in the cell nucleus and we observed that MAPKAPK-2 was phosphorylated (at Thr222) in the nucleus of the pre-osteoblast, mostly at 1 and 6 h of seeding. In the nature, multiple residues of MAPKAPK-2 are phosphorylated in response to distinct signaling pathways, however, only four residues (Thr25, Thr222, Ser272, and Thr334) can be phosphorylated by MAPKp38 [Ben-Levy et al., 1995]. Lastly, in order to evaluate the importance of MAPKp38 at early phase of pre-osteoblast adhesion, the adherent pre-osteoblasts were pre-treated with SB203580 (a synthetic p38 inhibitor) for 2 h. After treatment, the adherent cells were detached and re-seeded on another culture dish-plate. Intriguingly, this pre-treatment impaired pre-osteoblasts adhesion, about 50% of the cells failed to adhere but did not compromise these cells viability. This result provides evidence that MAPKp38 is a critical and crucial signaling protein for attachment of pre-osteoblasts, but new studies are necessary to address this process as well as to identify signaling proteins interacting with MAPKp38 during these events.

To our understanding, the elucidation of the molecular events triggered during adhesion and spreading of pre-osteoblasts are important to provide new insights for the improvement of cell-substratum interactions. It is expected that understanding the mechanisms of osteoblast adhesion, proliferation and differentiation are fundamental to design novel ''smart'' materials, enhancing integration of biomaterials within host tissue.

Although other investigators have assessed the ability of different surfaces to support primary osteoblast adhesion, growth, and differentiation, this is the first article, to our knowledge, that screens the time-course of molecular mechanisms responsible for actin-filaments remodeling at the beginning of pre-osteoblast adhesion, besides unraveling crucial details about it.

ACKNOWLEDGMENTS

WFZ is supported by a fellowship from Fundação de Amparo à Pesquisa do Estado de São Paulo (Grant nr. 08/53003-9). Also, the authors are grateful to Lab Technicians from Department of Cell Biology, University of Groningen, The Netherlands, and Department of Biochemistry, University of Campinas, Brazil, for excellent technical support.

REFERENCES

Adamson P, Paterson HF, Hall A. 1992. Intracellular localization of the p21rho proteins. J Cell Biol 119:617–627.

Ben-Levy R, Leighton IA, Doza YN, Attwood P, Morrice N, Marshall CJ, Cohen P. 1995. Identification of novel phosphorylation sites required for activation of MAPKAP kinase-2. EMBO J 14:5920–5930.

Bertazzo S, Zambuzzi WF, da Silva HA, Ferreira CV, Bertran CA. 2009. Bioactivation of alumina by surface modification: A possibility for improving the applicability of alumina in bone and oral repair. Clin Oral Impl Res 20:288–293.

Brasaemle DL, Attie AD. 1988. Microelisa reader quantitation of fixed, stained, solubilized cells in microtitre dishes. Biotechniques 6:418–419.

Carlier MF, Ressad F, Pantaloni D. 1999. Control of actin dynamics in cell motility. Role of ADF/cofilin. J Biol Chem 274:33827–33830.

Chen J, Martin BL, Brautigan DL. 1992. Regulation of protein serine-threonine phosphatase type-2A by tyrosine phosphorylation. Science 257: 1261–1264.

Choi MG, Koh HS, Kluess D, O'Connor D, Mathur A, Truskey GA, Rubin J, Zhou DX, Sung KL. 2005. Effects of titanium particle size on osteoblast functions in vitro and in vivo. Proc Natl Acad Sci USA 102:4578–4583.

Condeelis J. 2001. How is actin polymerization nucleated in vivo? Trends Cell Biol 11:288–293.

Ferreira CV, Justo GZ, Souza AC, Queiroz KC, Zambuzzi WF, Aoyama H, Peppelenbosch MP. 2006. Natural compounds as a source of protein tyrosine phosphatase inhibitors: Application to the rational design of small-molecule derivatives. Biochimie 88:1859–1873.

Fincham VJ, James M, Frame MC, Winder SJ. 2000. Active ERK/MAP kinase is targeted to newly forming cell-matrix adhesions by integrin engagement and v-Src. EMBO J 19:2911–2923.

Hamilton DW, Brunette DM. 2007. The effect of substratum topography on osteoblast adhesion mediated signal transduction and phosphorylation. Biomaterials 28:1806–1819.

Hartree EF. 1972. Determination of proteins: A modification of Lowry method that give a linear photometric response. Anal Biochem 48:422–427.

Kneser U, Stangenberg L, Ohnolz J, Buettner O, Stern-Straeter J, Möbest D, Horch RE, Stark GB, Schaefer DJ. 2006. Evaluation of processed bovine cancellous bone matrix seeded with syngenic osteoblasts in a critical size calvarial defect rat model. J Cell Mol Med 10:695–707.

Lavoie JN, Hickey E, Weber LA, Landry J. 1993. Modulation of actin microfilament dynamics and fluid phase pinocytosis by phosphorylation of heat shock protein 27. J Biol Chem 268:24210–24214.

Logeart-Avramoglou D, Anagnostou F, Bizios R, Petite H. 2005. Engineering bone: Challenges and obstacles. J Cell Mol Med 9:72–84.

Mosmann T. 1983. Rapid colorimetric assay for cellular growth and survival: Application to proliferation and cytotoxicity assay. J Immunol Meth 65:55–63.

Müller P, Bulnheim U, Diener A, Lüthen F, Teller M, Klinkenberg ED, Neumann HG, Nebe B, Liebold A, Steinhoff G, Rychly J. 2008. Calcium phosphate surfaces promote osteogenic differentiation of mesenchymal stem cells. J Cell Mol Med 12:281–291.

Myers KR, Casanova JE. 2008. Regulation of actin cytoskeleton dynamics by Arf-family GTPases. Trends Cell Biol 18:184–192.

Paterson HF, Self AJ, Garrett MD, Just I, Aktories K, Hall A. 1990. Microinjection of recombinant p21rho induces rapid changes in cell morphology. J Cell Biol 111:1001–1007.

Ridley AJ, Hall A. 1992. The small GTP-binding protein rhoA regulates the assembly of focal adhesions anad actin stress fibers in response to growth factors. Cell 70:389–399.

Rousseau S, Houle F, Landry J, Huot J. 1997. p38 MAP kinase activation by vascular endothelial growth factor mediates actin reorganization and cell migration in human endothelial cells. Oncogene 15:2169–2177.

Zambuzzi WF, Granjeiro JM, Parikh K, Yuvaraj S, Peppelenbosch MP, Ferreira CV. 2008. Modulation of Src activity by low molecular weight protein tyrosine phosphatase during osteoblast differentiation. Cell Physiol Biochem 22:497–506.

Zambuzzi WF, Yano CL, Cavagis AD, Peppelenbosch MP, Granjeiro JM, Ferreira CV. 2009. Ascorbate-induced osteoblast differentiation recruits distinct MMP-inhibitors: RECK and TIMP-2. Mol Cell Biochem 322:143–150.